Monte Carlo simulations in generalized isobaric-isothermal ensembles

Hisashi Okumura[1,2,*] and Yuko Okamoto[1,2,†]
[1]*Department of Theoretical Studies, Institute for Molecular Science, Okazaki, Aichi 444-8585, Japan*
[2]*Departments of Functional and Structural Molecular Science, The Graduate University for Advanced Studies, Okazaki, Aichi 444-8585, Japan*
(Received 3 February 2004; published 13 August 2004)

We present three generalized isobaric-isothermal ensemble Monte Carlo algorithms, which we refer to as the multibaric-multithermal, multibaric-isothermal, and isobaric-multithermal algorithms. These Monte Carlo simulations perform random walks widely in volume space and/or in potential energy space. From only one simulation run, one can calculate isobaric-isothermal-ensemble averages in wide ranges of pressure and temperature. We demonstrate the effectiveness of these algorithms by applying them to the Lennard-Jones 12-6 potential system with 500 particles.

DOI: 10.1103/PhysRevE.70.026702 PACS number(s): 05.10.−a, 02.70.Ns, 64.70.Fx, 47.55.Dz

I. INTRODUCTION

In statistical mechanics, various ensembles are considered. The Monte Carlo (MC) algorithm is an indispensable tool in computational statistical mechanics. In order to realize desired statistical ensembles, corresponding MC techniques have been developed [1–5]. The first MC simulation was performed in the canonical ensemble by Metropolis *et al.* [1], and it is still the most widely used ensemble. The isobaric-isothermal (ISOBATH) [2] and the microcanonical ensemble MC methods [3] are also extensively used.

Besides the above physical ensembles, it is now almost a default to simulate in artificial, generalized ensembles so that the multiple-minima problem, or the broken ergodicity problem, in complex systems can be overcome (for recent reviews, see Refs. [6–8]). The multicanonical algorithm [9,10] is one of the most well-known such methods in generalized ensemble. In a multicanonical ensemble, a non-Boltzmann weight factor is used so that a free 1D random walk is realized in the potential energy space. This enables the simulation to escape from any local-minimum-energy state and to sample the configurational space more widely than the conventional canonical MC algorithm. Another advantage is that one can obtain various canonical-ensemble averages in a wide range of temperatures from one simulation run by the reweighting techniques [11]. The generalized-ensemble algorithms are now widely used not only for simple systems but also for complex systems, such as proteins and glasses.

In the preceding letter [12], we proposed an MC algorithm in which one can obtain various ISOBATH ensembles from only one simulation run. In other words, we discussed bringing the multicanonical technique into the ISOBATH MC method. We refer to this method as the multibaric-multithermal (MUBATH) algorithm. This MC simulation performs a random walk in 2D space: volume space as well as potential energy space. There also exist a few works of multidimensional extensions of the multicanonical algorithm [13–19]. However, there has been no attempt to introduce the multicanonical idea into the ISOBATH ensemble.

In this article, we further introduce two variations of the MUBATH algorithm. In the two variations, simulations perform random walks either in volume space or in potential energy space. We refer to the former as the multibaric-isothermal (MUBA) algorithm and the latter as the isobaric-multithermal (MUTH) algorithm.

The above three methods have the following advantages: (i) They allow the simulations to escape from any local-minimum-energy state and to sample the configurational space more widely than the conventional ISOBATH method. One can know the most stable configuration at the designated pressure and temperature. (ii) One can obtain various ISOBATH ensembles from only one simulation run. (iii) One can control pressures and temperatures similarly to real experimental conditions. This method enables one to compare simulation conditions and those of experiments more easily and directly.

The outline of the present paper is as follows: In Sec. II we first review briefly the recently proposed MUBATH algorithm [12] and explain the MUBA algorithm and the MUTH algorithm. In Sec. III we present the computational details for the applications of these methods to the Lennard-Jones 12-6 potential system. In Sec. IV the results and discussions are presented, and concluding remarks follow in Sec. V.

II. METHODS

A. MUBATH algorithm

The probability distribution $\mathrm{P}_{NVT}(E;T_0)$ for potential energy E in the canonical ensemble at absolute temperature T_0 is given by the product of the density of states $n(E)$ and the Boltzmann weight factor $\mathrm{e}^{-\beta_0 E}$:

$$\mathrm{P}_{NVT}(E;T_0) = n(E)\mathrm{e}^{-\beta_0 E}, \tag{1}$$

where $\beta_0 = 1/k_\mathrm{B}T_0$ and k_B is the Boltzmann constant. Because $n(E)$ is a rapidly increasing function and the Boltzmann factor decreases exponentially, $\mathrm{P}_{NVT}(E;T_0)$ is a bell-shaped distribution.

*Electronic address: hokumura@ims.ac.jp
†Electronic address: okamotoy@ims.ac.jp

In the ISOBATH ensemble, on the other hand, both potential energy E and volume V fluctuate. The distribution $\mathrm{P}_{NPT}(E,V;T_0,P_0)$ for E and V at temperature T_0 and pressure P_0 is given by

$$\mathrm{P}_{NPT}(E,V;T_0,P_0) = n(E,V)\mathrm{e}^{-\beta_0 H}, \tag{2}$$

where the density of states $n(E,V)$ is given as a function of E as well as V, and H is the "enthalpy" (without the kinetic-energy contributions):

$$H = E + P_0 V. \tag{3}$$

This ensemble yields a bell-shaped distribution in both E and V, while the canonical ensemble gives such a distribution only in E.

The conventional ISOBATH MC simulations are performed as follows [2]. The partition function Y_{NPT} in the ISOBATH ensemble is given by

$$Y_{NPT} = \frac{1}{\Lambda^{3N} N!}\int_0^\infty dV \int d\boldsymbol{r}^{(N)}\mathrm{e}^{-\beta_0 H}, \tag{4}$$

where Λ is the thermal de Broglie wavelength, N is the total number of particles of the system, and $\boldsymbol{r}^{(N)}=\{\boldsymbol{r}_1,\cdots,\boldsymbol{r}_N\}$ are real coordinates of the particles. Introducing scaled coordinates $\boldsymbol{s}_i=L^{-1}\boldsymbol{r}_i$ (here, the particles are placed in a cubic box of a side of size $L\equiv\sqrt[3]{V}$), the above equation is rewritten as

$$Y_{NPT} = \frac{1}{\Lambda^{3N} N!}\int_0^\infty dV \int d\boldsymbol{s}^{(N)}\mathrm{e}^{-\beta_0(H-Nk_\mathrm{B}T_0\ln V)}, \tag{5}$$

where the enthalpy is now a function of $\boldsymbol{s}^{(N)}$ and V:

$$H = H[E(\boldsymbol{s}^{(N)},V),V] = E[\boldsymbol{s}^{(N)},V] + P_0 V. \tag{6}$$

Therefore, the probability density $\mathcal{N}[\boldsymbol{s}^{(N)},V]$ that the system has a specific configuration $\boldsymbol{s}^{(N)}$ in a volume V is given by

$$\mathcal{N}[\boldsymbol{s}^{(N)},V] \propto \mathrm{e}^{-\beta_0\{H-Nk_\mathrm{B}T_0\ln V\}}. \tag{7}$$

We can now perform Metropolis sampling on the scaled coordinates $\boldsymbol{s}^{(N)}$ and the volume V. The trial moves of the coordinates from $\boldsymbol{s}_i$ to $\boldsymbol{s}_i{}'$ and of the volume from V to V' are generated by uniform random numbers. The enthalpy is consequently changed from $H\{E[\boldsymbol{s}^{(N)},V],V\}$ to $H' \equiv H\{E[\boldsymbol{s}^{(N)\prime},V'],V'\}$ by these trial moves. According to Eq. (7), the trial moves will now be accepted by the Metropolis criterion with the probability

$$w(\mathrm{o}\rightarrow\mathrm{n}) = \min(1,\exp[-\beta_0\{H' - H - Nk_\mathrm{B}T_0\ln(V'/V)\}]). \tag{8}$$

The ISOBATH probability distribution $\mathrm{P}_{NPT}(E,V;T_0,P_0)$ is obtained by this scheme.

In this paper we introduce three versions of multicanonical extensions of the ISOBATH ensemble (two of them will be presented in the next subsections). In the multicanonical ensemble, a non-Boltzmann weight factor $W_\mathrm{mc}(E)$ is used. This multicanonical weight factor is characterized by a flat probability distribution $\mathrm{P}_\mathrm{mc}(E)$:

$$\mathrm{P}_\mathrm{mc}(E) = n(E)W_\mathrm{mc}(E) = \mathrm{const}, \tag{9}$$

and thus a free random walk is realized in the potential energy space.

The first example is the MUBATH ensemble, where simulations perform random walks in both potential energy space and volume space. For the purpose of realizing such random walks, every state is sampled by the MUBATH weight factor $W_\mathrm{mbt}(E,V)$ so that a uniform distribution in both potential energy space and volume space may be obtained:

$$\mathrm{P}_\mathrm{mbt}(E,V) = n(E,V)W_\mathrm{mbt}(E,V) \equiv n(E,V)\exp\{-\beta_0 H_\mathrm{mbt}(E,V)\} = \mathrm{const}, \tag{10}$$

where H_mbt is referred to as the MUBATH enthalpy.

In order to perform the MUBATH MC simulation, we follow the conventional ISOBATH MC techniques as described above. Namely, the trial moves of the coordinates from $\boldsymbol{s}_i$ to $\boldsymbol{s}_i{}'$ and of the volume from V to V' are generated by uniform random numbers. The MUBATH enthalpy is consequently changed from $H_\mathrm{mbt}\{[E(\boldsymbol{s}^{(N)},V],V\}$ to $H'_\mathrm{mbt} \equiv H_\mathrm{mbt}\{E[\boldsymbol{s}^{(N)\prime},V'],V'\}$ by these trial moves. By replacing H by H_mbt in Eq. (8), the trial moves will now be accepted with the probability

$$w(\mathrm{o}\rightarrow\mathrm{n}) = \min(1,\exp[-\beta_0\{H'_\mathrm{mbt} - H_\mathrm{mbt} - Nk_\mathrm{B}T_0\ln(V'/V)\}]). \tag{11}$$

The MUBATH weight factor is, however, not *a priori* known and has to be determined by the usual iterations of short simulations [20–22]. The first simulation is carried out at T_0 and P_0 in the ISOBATH ensemble. Namely, we use

$$W^{(1)}_\mathrm{mbt}(E,V) = \exp\{-\beta_0 H^{(1)}_\mathrm{mbt}(E,V)\}, \tag{12}$$

where

$$H^{(1)}_\mathrm{mbt}(E,V) = E + P_0 V. \tag{13}$$

The $(i-1)$th simulation is performed with the weight factor $W^{(i-1)}_\mathrm{mbt}(E,V)$ and let $\mathrm{P}^{(i-1)}_\mathrm{mbt}(E,V)$ be the obtained distribution. The ith weight factor $W^{(i)}_\mathrm{mbt}(E,V)$ is then given by

$$W^{(i)}_\mathrm{mbt}(E,V) = \exp[-\beta_0 H^{(i)}_\mathrm{mbt}(E,V)], \tag{14}$$

where

$$H^{(i)}_{\mathrm{mbt}}(E,V) = \begin{cases} H^{(i-1)}_{\mathrm{mbt}}(E,V) + k_{\mathrm{B}}T_0 \ln \mathrm{P}^{(i-1)}_{\mathrm{mbt}}(E,V), & \text{for} \quad \mathrm{P}^{(i-1)}_{\mathrm{mbt}}(E,V) > 0, \\ H^{(i-1)}_{\mathrm{mbt}}(E,V), & \text{for} \quad \mathrm{P}^{(i-1)}_{\mathrm{mbt}}(E,V) = 0. \end{cases} \tag{15}$$

For convenience, we discretize E and V into bins and use histograms to calculate $\mathrm{P}^{(i)}_{\mathrm{mbt}}(E,V)$. We iterate this process until a reasonably flat distribution $\mathrm{P}^{(i)}_{\mathrm{mbt}}(E,V)$ is obtained.

After an optimal weight factor $W_{\mathrm{mbt}}(E,V)$ is determined, a long production simulation is performed for data collection. We can apply the reweighting techniques [11] to the results of this production run in order to calculate the ISOBATH ensemble averages at the designated temperature T and pressure P. Namely, the probability distribution $\mathrm{P}_{NPT}(E,V;T,P)$ in the ISOBATH ensemble in wide ranges of T and P is given by

$$\mathrm{P}_{NPT}(E,V;T,P) = \frac{\mathrm{P}_{\mathrm{mbt}}(E,V)W^{-1}_{\mathrm{mbt}}(E,V)\mathrm{e}^{-\beta(E+PV)}}{\int dV \int dE\ \mathrm{P}_{\mathrm{mbt}}(E,V)W^{-1}_{\mathrm{mbt}}(E,V)\mathrm{e}^{-\beta(E+PV)}}. \tag{16}$$

The expectation value of a physical quantity A at T and P is obtained from

$$\langle A\rangle_{NPT} = \int dV \int dE\ A(E,V)\mathrm{P}_{NPT}(E,V;T,P) = \frac{\langle A(E,V)W^{-1}_{\mathrm{mbt}}(E,V)\mathrm{e}^{-\beta(E+PV)}\rangle_{\mathrm{mbt}}}{\langle W^{-1}_{\mathrm{mbt}}(E,V)\mathrm{e}^{-\beta(E+PV)}\rangle_{\mathrm{mbt}}}, \tag{17}$$

where $\langle\cdots\rangle_{\mathrm{mbt}}$ is the MUBATH ensemble average.

B. MUBA algorithm

The second example of multicanonical extensions of the ISOBATH ensemble is the MUBA ensemble. Simulations in this ensemble perform random walks in the volume space. For obtaining the volume-space random walk, the ISOBATH weight factor $\mathrm{e}^{-\beta_0(E+P_0V)}$ is changed partially. That is, the energy part $\mathrm{e}^{-\beta_0 E}$ is used as it is, and the volume part $\mathrm{e}^{-\beta_0 P_0 V}$, on the other hand, is modified into $W_{\mathrm{mb}}(V) \equiv \exp[-\beta_0\Omega_{\mathrm{mb}}(V)]$ so that a flat probability distribution in volume may be obtained:

$$\mathrm{P}_{\mathrm{mb}}(E,V) = n(E,V)\exp[-\beta_0 E]W_{\mathrm{mb}}(V) = n(E,V)\exp[-\beta_0\{E+\Omega_{\mathrm{mb}}(V)\}] = \text{const on } V. \tag{18}$$

We refer to $W_{\mathrm{mb}}(V)$ as the MUBA weight factor. The trial moves are performed on $\boldsymbol{s}_i$ and V as in the above algorithms. These trial moves will be accepted with the probability [see Eq. (11)]

$$\mathrm{acc}(\mathrm{o}\to\mathrm{n}) = \min(1,\exp[-\beta_0\{E'-E+\Omega_{\mathrm{mb}}(V')-\Omega_{\mathrm{mb}}(V) - Nk_{\mathrm{B}}T_0\ln(V'/V)\}]). \tag{19}$$

Note that substituting $E+\Omega_{\mathrm{mb}}(V)$ by $H_{\mathrm{mbt}}(E,V)$, Eq. (19) returns to that of the MUBATH algorithm [Eq. (11)].

The MUBA weight factor $W_{\mathrm{mb}}(V)$ has to be determined again by the usual iterations of short simulations [20–22]. The probability distribution in the volume space

$$\tilde{\mathrm{P}}_{\mathrm{mb}}(V) \equiv \int dE\ \mathrm{P}_{\mathrm{mb}}(E,V) \tag{20}$$

is calculated during the MUBA simulation iterations, whereas the probability distribution $\mathrm{P}_{\mathrm{mbt}}(E,V)$ is calculated in the 2D $E-V$ space in the MUBATH simulations. The weight factor $W^{(i)}_{\mathrm{mb}}(V)$ at the ith simulation is determined by

$$W^{(i)}_{\mathrm{mb}}(V) = \exp[-\beta_0\Omega^{(i)}_{\mathrm{mb}}(V)], \tag{21}$$

where

$$\Omega^{(1)}_{\mathrm{mb}}(V) = P_0V \tag{22}$$

for the first ISOBATH simulation ($i=1$) or

$$\Omega^{(i)}_{\mathrm{mb}}(V) = \begin{cases} \Omega^{(i-1)}_{\mathrm{mb}}(V) + k_{\mathrm{B}}T_0 \ln \tilde{\mathrm{P}}^{(i-1)}_{\mathrm{mb}}(V), & \text{for} \quad \tilde{\mathrm{P}}^{(i-1)}_{\mathrm{mb}}(V) > 0, \\ \Omega^{(i-1)}_{\mathrm{mb}}(V), & \text{for} \quad \tilde{\mathrm{P}}^{(i-1)}_{\mathrm{mb}}(V) = 0 \end{cases} \tag{23}$$

for $i \geqslant 2$. Here, $\tilde{\mathrm{P}}^{(i-1)}_{\mathrm{mb}}(V)$ is the obtained distribution of volume at the $(i-1)$th simulation.

After an optimal weight factor $W_{\mathrm{mb}}(V)$ is determined, a long production simulation is performed. We use the reweighting techniques to calculate the ISOBATH ensemble averages at chosen values of T and P. The probability distribution $\mathrm{P}_{NPT}(E,V;T,P)$ is given by

$$\mathrm{P}_{NPT}(E,V;T,P) = \frac{\mathrm{P}_{\mathrm{mb}}(E,V)W^{-1}_{\mathrm{mb}}(V)\mathrm{e}^{-\beta PV}\mathrm{e}^{-(\beta-\beta_0)E}}{\int dV \int dE\ \mathrm{P}_{\mathrm{mb}}(E,V)W^{-1}_{\mathrm{mb}}(V)\mathrm{e}^{-\beta PV}\mathrm{e}^{-(\beta-\beta_0)E}}. \tag{24}$$

The expectation value of a physical quantity A at T and P is obtained from

$$\langle A\rangle_{NPT} = \frac{\langle A(E,V)W^{-1}_{\mathrm{mb}}(V)\mathrm{e}^{-\beta PV}\mathrm{e}^{-(\beta-\beta_0)E}\rangle_{\mathrm{mb}}}{\langle W^{-1}_{\mathrm{mb}}(V)\mathrm{e}^{-\beta PV}\mathrm{e}^{-(\beta-\beta_0)E}\rangle_{\mathrm{mb}}}, \tag{25}$$

where $\langle\cdots\rangle_{\mathrm{mb}}$ means the MUBA ensemble average. The energy part still remains $\mathrm{e}^{-\beta_0 E}$ as in the ISOBATH method in Eq. (18), i.e., the temperature is fixed at T_0 during the simulation. This means that the configurational space is not sampled widely in the energy space. Therefore, the reweighting techniques are employed only at a temperature that is close to T_0:

$$T \approx T_0. \tag{26}$$

However, due to the volume part $e^{-\beta_0 \Omega_{mb}(V)}$, one can sample a wide volume space and calculate the distribution $P_{NPT}(E,V;T,P)$ in the wide range of P/T or P.

C. MUTH algorithm

The third example of multicanonical extensions of the ISOBATH ensemble is the MUTH ensemble. Simulations in this ensemble perform random walks in the potential energy space, while the volume-space random walk is realized in the MUBA algorithm of the previous subsection. For obtaining the energy-space random walk, the ISOBATH weight factor $e^{-\beta_0(E+P_0V)}$ is again changed partially. That is, the volume part $e^{-\beta_0 P_0 V}$ is used as it is, and the energy part $e^{-\beta_0 E}$ is modified into $W_{mt}(E) \equiv \exp[-\beta_0 E_{mt}(E)]$ so that a flat probability distribution in the potential energy space may be obtained:

$$\begin{aligned} P_{mt}(E,V) &= n(E,V)\exp[-\beta_0 P_0 V] W_{mt}(E) \\ &= n(E,V)\exp[-\beta_0\{E_{mt}(E) + P_0 V\}] = \text{const on } E. \end{aligned} \tag{27}$$

We refer to $W_{mt}(E)$ as the MUTH weight factor. The trial moves of $\boldsymbol{s}_i$ and V will be accepted with the probability

$$\begin{aligned} \mathrm{acc}(o \to n) = \min(1, \exp[&-\beta_0\{E'_{mt} - E_{mt} + P_0(V' - V) \\ &- N k_B T_0 \ln(V'/V)\}]). \end{aligned} \tag{28}$$

Note that substituting $E_{mt}(E) + P_0 V$ by $H_{mbt}(E,V)$, Eq. (28) returns to that of the MUBATH algorithm [Eq. (11)].

The MUTH weight factor $W_{mt}(E)$ is also determined by the usual iterations of short simulations [20–22]. The probability distribution in the potential energy space

$$\tilde{P}_{mt}(E) \equiv \int dV\, P_{mt}(E,V) \tag{29}$$

is calculated during the iterations. The weight factor $W_{mt}^{(i)}(E)$ at the ith simulation is determined by

$$W_{mt}^{(i)}(E) = \exp[-\beta_0 E_{mt}^{(i)}(E)], \tag{30}$$

where

$$E_{mt}^{(1)}(E) = E \tag{31}$$

at the first ISOBATH simulation ($i=1$) or

$$E_{mt}^{(i)}(E) = \begin{cases} E_{mt}^{(i-1)}(E) + k_B T_0 \ln \tilde{P}_{mt}^{(i-1)}(E), & \text{for} \quad \tilde{P}_{mt}^{(i-1)}(E) > 0, \\ E_{mt}^{(i-1)}(E), & \text{for} \quad \tilde{P}_{mt}^{(i-1)}(E) = 0 \end{cases} \tag{32}$$

for $i \geq 2$. Here, $\tilde{P}_{mt}^{(i-1)}(E)$ is the obtained distribution at the $(i-1)$th simulation.

After an optimal weight factor is determined, a long production simulation is performed. In order to calculate the ISOBATH ensemble averages, we use the reweighting techniques and calculate the distribution $P_{NPT}(E,V;T,P)$ at chosen values of T and P as follows:

$$P_{NPT}(E,V;T,P) = \frac{P_{mt}(E,V) W_{mt}^{-1}(E) e^{-\beta E} e^{-(\beta P - \beta_0 P_0)V}}{\int dV \int dE\, P_{mt}(E,V) W_{mt}^{-1}(E) e^{-\beta E} e^{-(\beta P - \beta_0 P_0)V}}. \tag{33}$$

The expectation value of a physical quantity A at T and P is then obtained from

$$\langle A \rangle_{NPT} = \frac{\langle A(E,V) W_{mt}^{-1}(E) e^{-\beta E} e^{-(\beta P - \beta_0 P_0)V} \rangle_{mt}}{\langle W_{mt}^{-1}(E) e^{-\beta E} e^{-(\beta P - \beta_0 P_0)V} \rangle_{mt}}, \tag{34}$$

where $\langle \cdots \rangle_{mt}$ means the MUTH ensemble average. However, in the present case, we have the following restrictions on the range of values of T and P which we can choose

$$\frac{P}{T} \approx \frac{P_0}{T_0}. \tag{35}$$

This is because the volume part remains as $e^{-\beta_0 P_0 V}$ in Eq. (27), i.e., the pressure-temperature ratio P/T is fixed at P_0/T_0 during the simulation. This means that the configurational space is not sampled widely in the volume space. Therefore, the reweighting techniques are employed only at P and T whose P/T is close to P_0/T_0. On the other hand, the energy space is sampled widely thus one can calculate the distribution $P_{NPT}(E,V;T,P)$ and the average quantities in the wide range of T. Here, we should note that the conjugate variable for V is P/T, rather than P, and the conjugate variable for E is $1/T$, that is, T.

III. COMPUTATIONAL DETAILS

We now give the details of our simulations. We consider a Lennard-Jones 12-6 potential system. The length and the energy are scaled in units of the Lennard-Jones diameter σ and the depth of the potential ϵ, respectively. We use an asterisk (*) for the reduced quantities, such as the reduced length $r^* = r/\sigma$, the reduced temperature $T^* = k_B T/\epsilon$, and the reduced pressure $P^* = P\sigma^3/\epsilon$.

We used 500 particles ($N=500$) in a cubic unit cell with periodic boundary conditions. We started the weight-factor determination for the three generalized ISOBATH simulations from a regular ISOBATH simulation at $T_0^*=2.0$ and $P_0^*=3.0$. These temperature and pressure values are, respectively, higher than the critical temperature T_c^* and the critical pressure P_c^* [23–28]. Recent reliable data are $T_c^*=1.3207(4)$ and $P_c^*=0.1288(5)$ [28]. The cutoff radius r_c^* was taken to be $L^*/2$. A cutoff correction was added for the pressure and the potential energy. In one MC sweep, we made the trial moves of all particle coordinates and the volume ($N+1$ trial moves altogether). For each trial move the Metropolis evaluations of Eqs. (11), (19), and (28) were made for MUBATH, MUBA, and MUTH algorithms, respectively. In order to obtain flat probability distributions $P_{mbt}(E,V)$, $\tilde{P}_{mb}(V)$, and

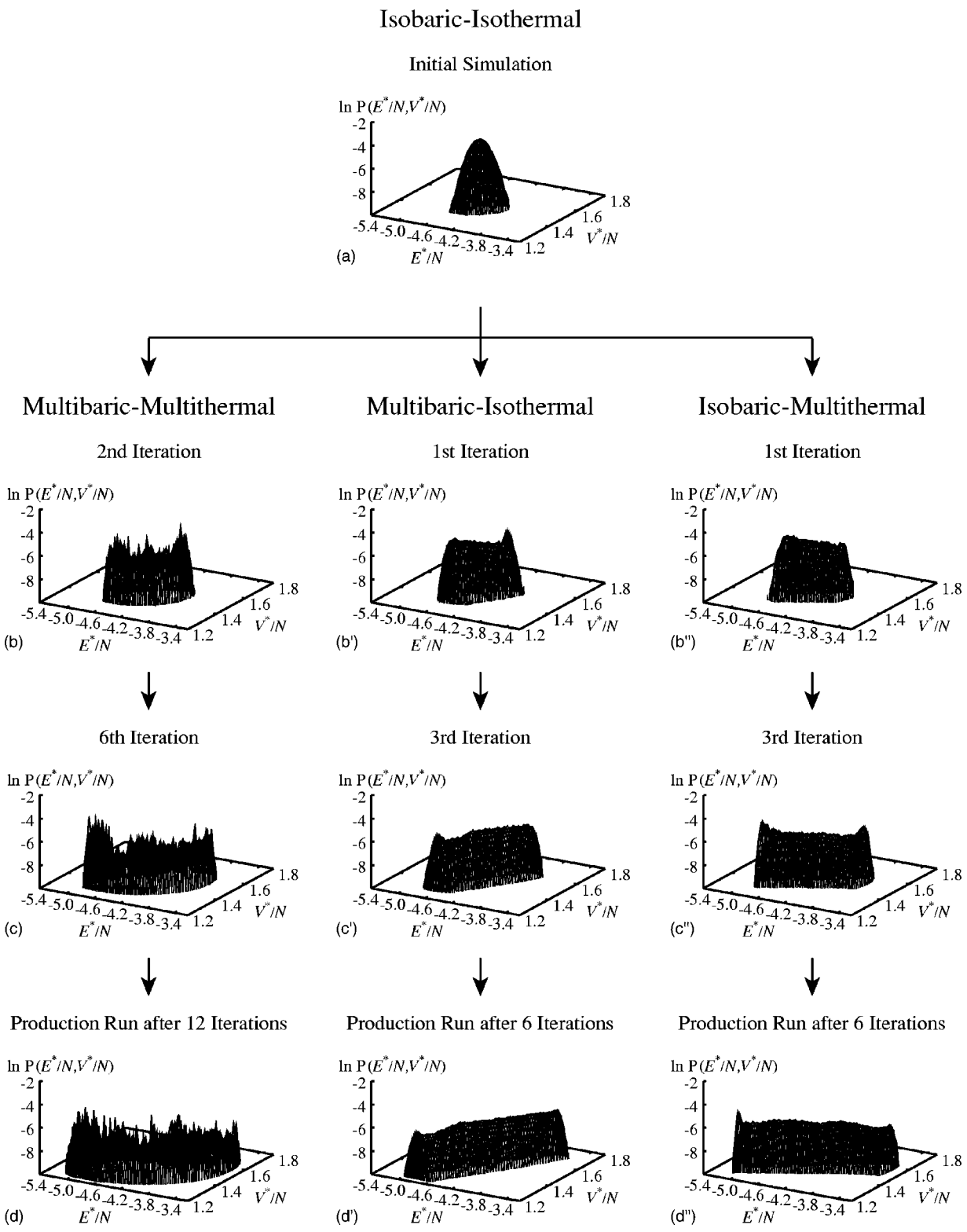

FIG. 1. The probability distributions $P(E^*/N, V^*/N)$ in logarithmic scale (a) from the ISOBATH simulation, (b)–(d) from the MUBATH simulations, (b′)–(d′) from the MUBA simulations, and (b″)–(d″) from the MUTH simulations.

$\tilde{P}_{mt}(E)$, we carried out relatively short MC simulations of 100 000 MC sweeps and iterated the processes of Eqs. (14) and (15), (21) and (23), and (30) and (32), respectively. In the present case, it was required to make 12 iterations to get an optimal MUBATH weight factor $W_{mbt}(E,V)$ and six iterations to obtain appropriate MUBA weight factor $W_{mb}(V)$ and MUTH weight factor $W_{mt}(E)$. We then performed a long production run of 400 000 MC sweeps with each of the three algorithms. We chose the bin sizes of these distributions $\Delta E^*/N=0.02$ and $\Delta V^*/N=0.01$ for MUBATH, $\Delta V^*/N$

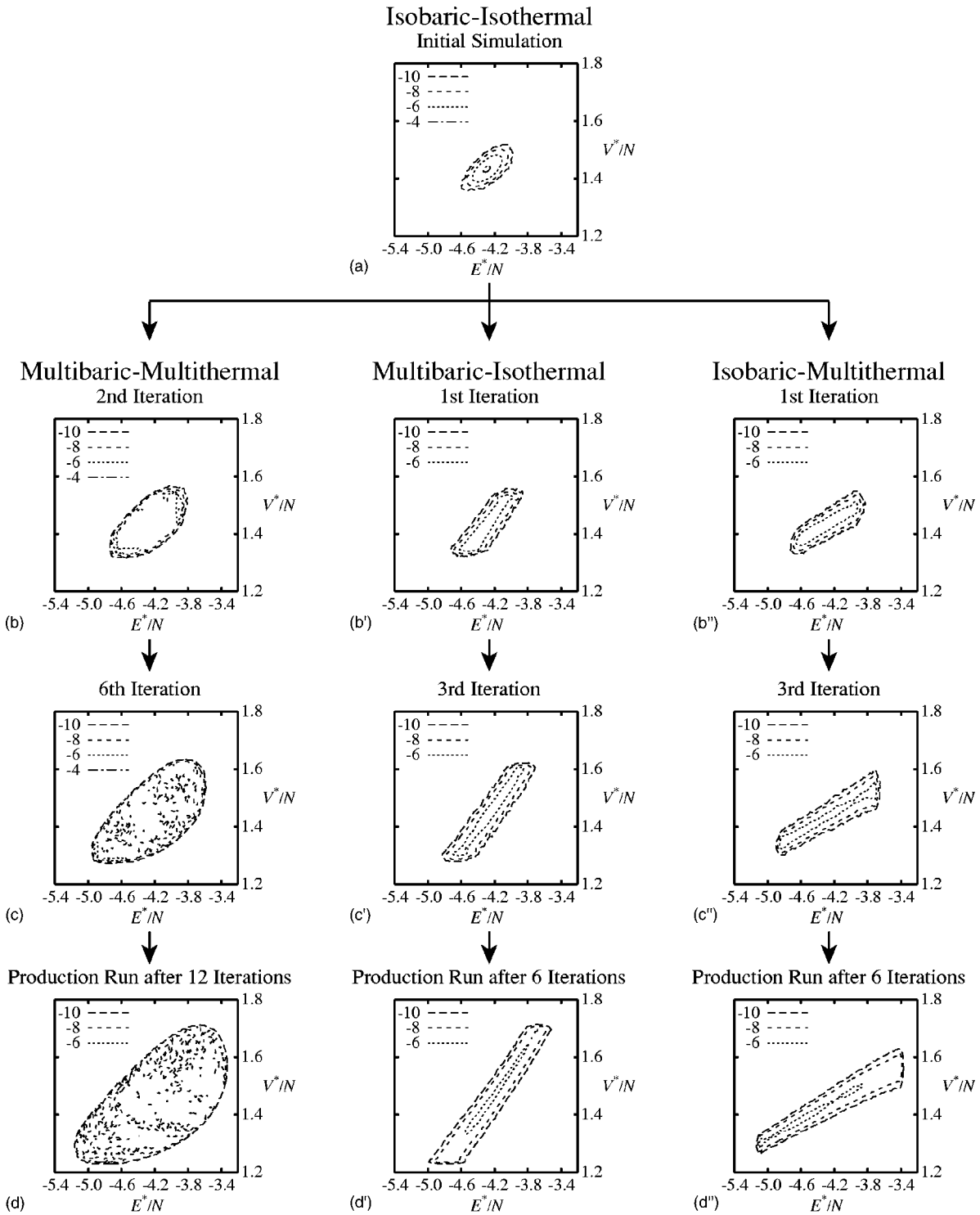

FIG. 2. The contour maps of the probability distributions $P(E^*/N, V^*/N)$ in logarithmic scale (a) from the ISOBATH simulation, (b)–(d) from the MUBATH simulations, (b′)–(d′) from the MUBA simulations, and (b″)–(d″) from the MUTH simulations.

$=0.005$ for MUBA, and $\Delta E^*/N=0.01$ for MUTH simulations.

For the purpose of comparisons of the new method to the conventional one, we also performed the ISOBATH MC simulations of 400 000 MC sweeps with 500 Lennard-Jones 12-6 potential particles at several sets of temperature and pressure values. They were carried out at $(T_0^*, P_0^*) = (2.0, 3.0)$, (1.6, 3.0), (2.4, 3.0), (2.0, 2.2), and (2.0, 3.8). The first set is the same as (T_0^*, P_0^*) that was used in the first iteration of the weight-factor determinations in the MUBATH, MUBA, and MUTH simulations [see Eqs. (12), (13), (21), (22), (27), and (30)].

In order to assess the statistical accuracies, we performed these MC simulations from four different initial conditions in

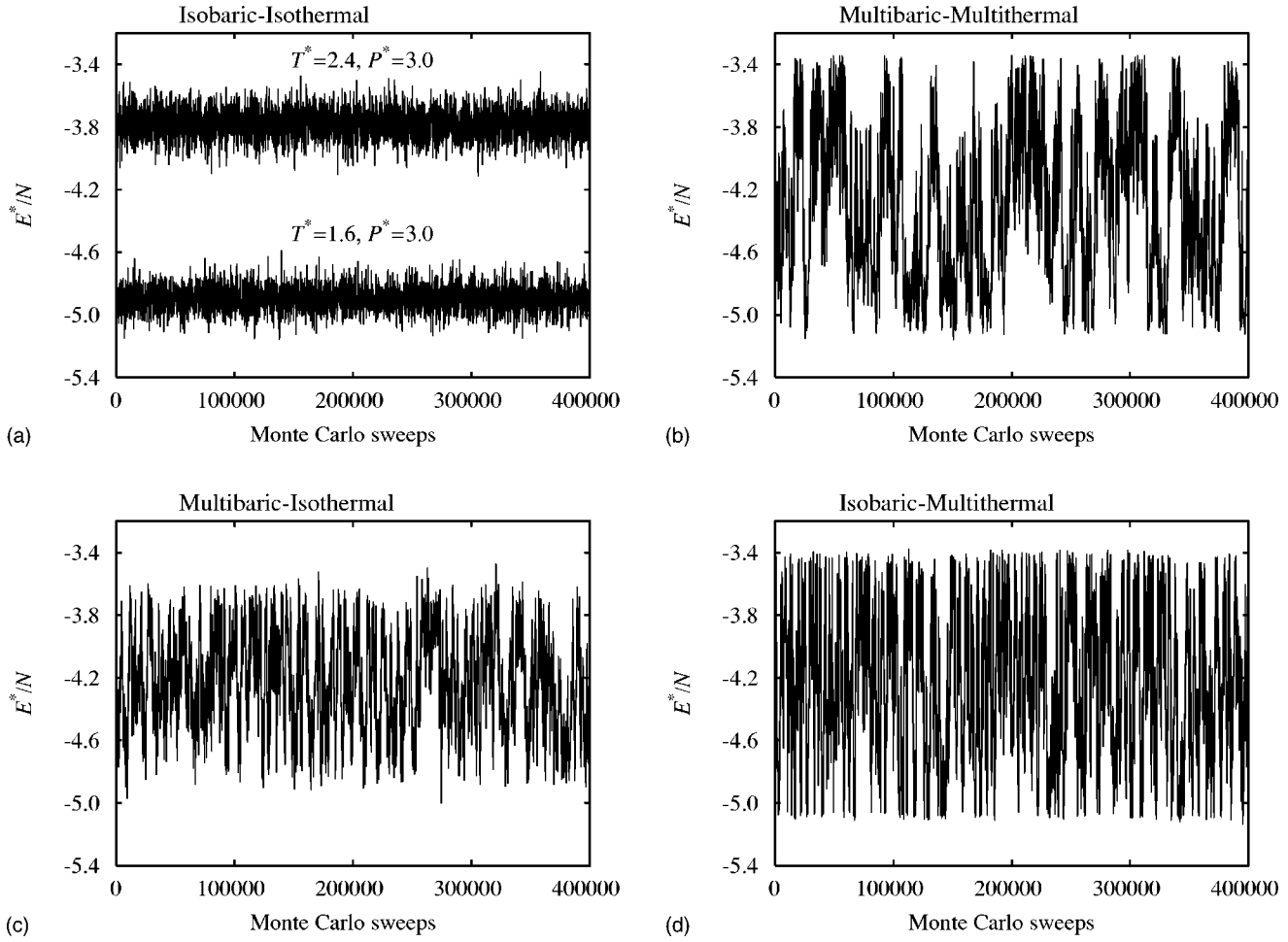

FIG. 3. The time series of E^*/N from (a) the ISOBATH MC simulations at $(T^*,P^*)=(2.4,3.0)$ and at $(T^*,P^*)=(1.6,3.0)$, (b) the MUBATH MC simulation, (c) the MUBA MC simulation, and (d) the MUTH MC simulation.

all the algorithms. The error bars were estimated by the standard deviations from these different simulations.

IV. RESULTS AND DISCUSSION

We now present the results of the MUBATH, MUBA, and MUTH simulations of the Lennard-Jones system of 500 particles. Figures 1 and 2 show the probability distributions of E^*/N and V^*/N in logarithmic scale and their contour maps, respectively. Figures 1(a) and 2(a) show $\mathrm{P}_{NPT}(E^*/N,V^*/N)$ from the ISOBATH simulation first carried out in the process of Eqs. (12) and (13) (i.e., $T_0^*=2.0$ and $P_0^*=3.0$). It is a bell-shaped distribution. As the iteration of Eqs. (14) and (15) in the MUBATH simulation proceeds, $\mathrm{P}_{\mathrm{mbt}}(E^*/N,V^*/N)$ will become flat and broad gradually as shown in Figs. 1(b)–1(d) and in Figs. 2(b)–2(d). This fact implies that the MUBATH MC simulation indeed sampled the configurational space in wider ranges of energy and volume than the conventional ISOBATH MC simulation.

Figures 1(b′)–1(d′) and 2(b′)–2(d′) show the probability distributions $\mathrm{P}_{\mathrm{mb}}(E^*/N,V^*/N)$ from the MUBA simulations. It is found that $\mathrm{P}_{\mathrm{mb}}(E^*/N,V^*/N)$ becomes gradually broad in the volume space like a ribbon with an almost fixed width of the potential-energy distribution by the iteration procedure of Eqs. (21) and (23). In the MUBA method, one can obtain various ISOBATH ensembles at various pressure values near temperature T_0^*. The distributions $\mathrm{P}_{\mathrm{mb}}(E^*/N,V^*/N)$ in Figs. 1(d′) and 2(d′) contain these ISOBATH-ensemble distributions. Comparing Figs. 1(d) and 2(d) with Figs. 1(d′) and 2(d′), the broadness in the volume space of the MUBA distribution after the six iterations is almost the same as that of the MUBATH distribution after the 12 iterations. That is, in order to obtain a broad distribution in the volume space, the MUBA simulation needs only about half a number of iterations when compared to the MUBATH simulation.

Figures 1(b″)–(d″) and 2(b″)–2(d″) show the probability distributions $\mathrm{P}_{\mathrm{mt}}(E^*/N,V^*/N)$ from the MUTH simulations. In contrast to the MUBA simulation, $\mathrm{P}_{\mathrm{mt}}(E^*/N,V^*/N)$ from the MUTH simulation becomes broad in the potential-energy space like a ribbon with an almost fixed width of the volume distribution by the iteration process of Eqs. (30) and (32). In the MUTH method, one can obtain various ISOBATH ensembles, in which the pressure-temperature ratios P^*/T^* are the same as P_0^*/T_0^*. The distributions $\mathrm{P}_{\mathrm{mt}}(E^*/N,V^*/N)$ in Figs. 1(d″) and 2(d″) contain these ISOBATH-ensemble distributions. The MUTH simulation after the six iterations makes a potential-energy distribution as broad as that of the

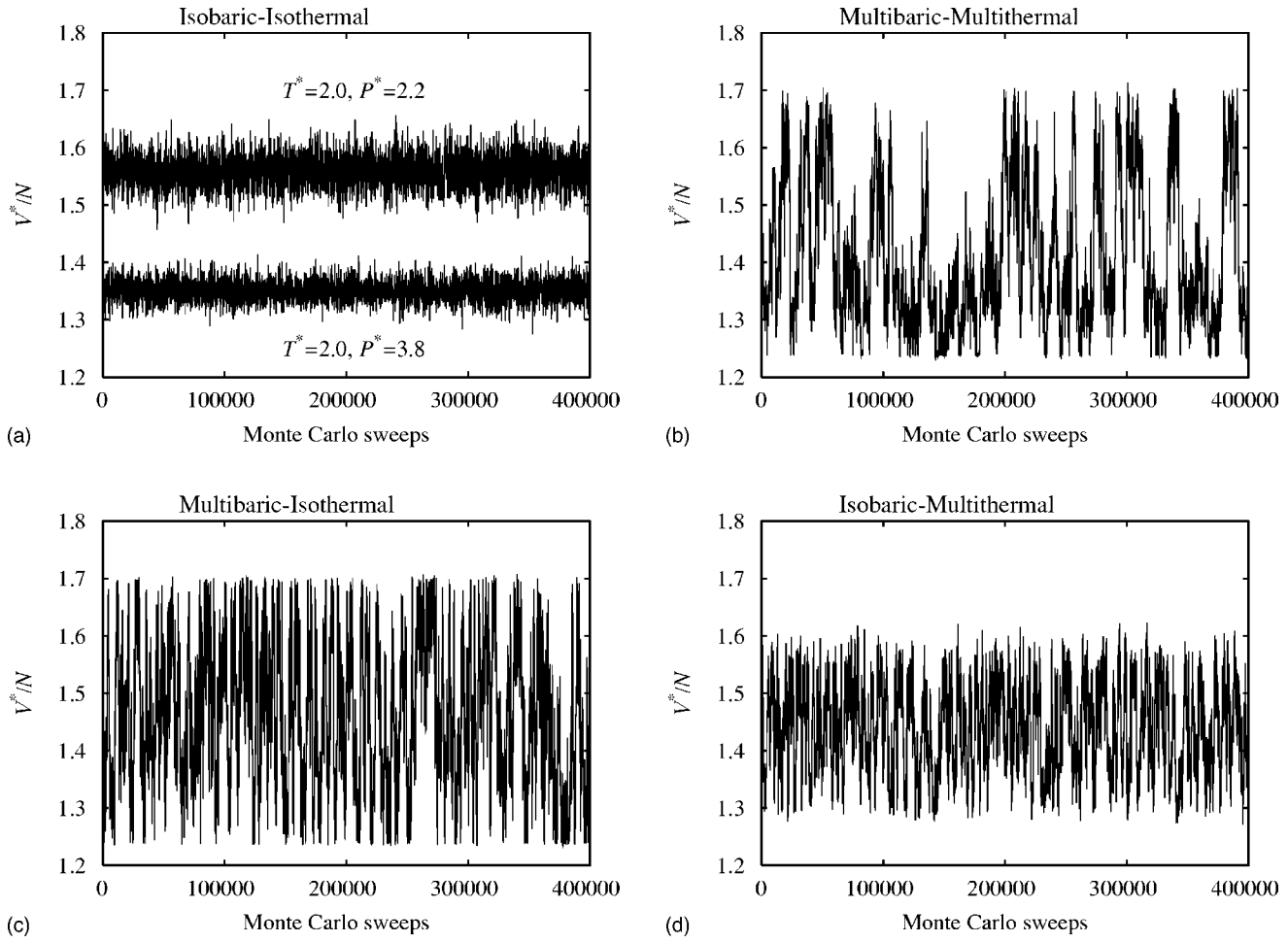

FIG. 4. The time series of V^*/N from (a) the ISOBATH MC simulations at $(T^*,P^*)=(2.0,3.8)$ and at $(T^*,P^*)=(2.0,2.2)$, (b) the MUBATH MC simulation, (c) the MUBA MC simulation, and (d) the MUTH MC simulation.

MUBATH simulation after the 12 iterations. For obtaining a wide distribution in the potential-energy space, about half the number of iterations is necessary in the MUTH simulation when compared to the MUBATH simulation. For a flat and broad distribution in both spaces, however, the MUBATH simulation is required.

Figure 3 shows the time series of E^*/N. Figure 3(a) gives the results from the conventional ISOBATH MC simulations at $(T^*,P^*)=(1.6,3.0)$ and (2.4, 3.0), while Fig. 3(b) presents those of the MUBATH simulation. The potential energy fluctuates in narrow ranges in the conventional ISOBATH simulations. They fluctuate only in the ranges of $E^*/N=-4.0\sim-3.6$ and $E^*/N=-5.1\sim-4.7$ at the higher temperature of $T^*=2.4$ and at the lower temperature of $T^*=1.6$, respectively. On the other hand, the MUBATH MC simulation performs a random walk that covers a wide energy range. A similar situation is observed in the MUTH simulation, which is illustrated in Fig. 3(d). The MUTH algorithm realizes a random walk in the potential energy space and covers a wide energy range. On the other hand, Fig. 3(c) implies that the MUBA algorithm samples the E^*/N space in the range much wider than the conventional ISOBATH simulation, but slightly narrower than the MUBATH and MUTH simulations. This is because the MUBA method is designed to realize a 1D random walk in the volume space rather than in the potential energy space. Moreover, the MUTH method is to realize only a 1D random walk in the potential-energy space, whereas the MUBATH algorithm has to perform a 2D random walk both in the potential-energy space and in the volume space. The random walk in the potential-energy space is therefore most efficient (most frequent visits to both the lowest and the highest energy values) in the MUTH simulation compared to the MUBATH and the MUBA simulations.

Figure 4 shows the time series of V^*/N. Figure 4(a) gives the results from the conventional ISOBATH simulations at $(T^*,P^*)=(2.0,3.8)$ and (2.0, 2.2), while Fig. 4(b) presents those of the MUBATH simulation. The volume fluctuates in narrow ranges in the conventional ISOBATH MC simulations. They fluctuate only in the ranges of $V^*/N=1.3\sim1.4$ and $V^*/N=1.5\sim1.6$ at the higher pressure of $P^*=3.8$ and at the lower pressure of $P^*=2.2$, respectively. On the other hand, the MUBATH simulation [Fig. 4(b)] and the MUBA simulation [Fig. 4(c)] perform random walks that cover a wide volume range. In contrast, Fig. 4(d) shows that the MUTH algorithm samples the V^*/N space in the range much wider than the conventional ISOBATH simulation, but slightly narrower than the MUBATH and MUBA simulations. This is because the MUTH algorithm is designed to

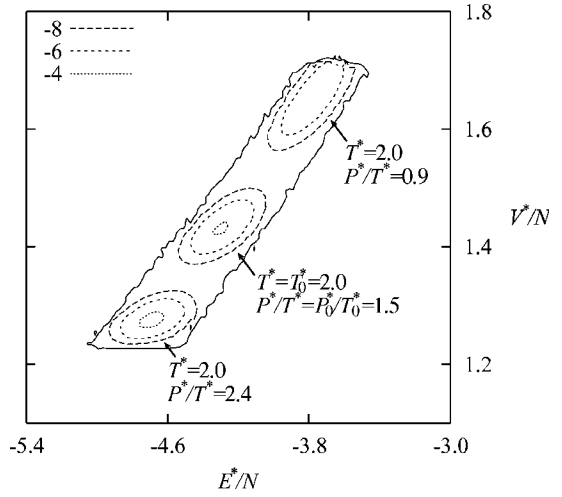

FIG. 5. The contour maps of the probability distributions $P_{NPT}(E^*/N, V^*/N; T^*, P^*)$ in logarithmic scale. They are determined from the MUBA MC simulation by the reweighting techniques at $(T^*, P^*/T^*) = (T_0^*, P_0^*/T_0^*) = (2.0, 1.5)$, $(T^*, P^*/T^*) = (2.0, 0.9)$, and $(T^*, P^*/T^*) = (2.0, 2.4)$. The outer solid curve is the contour map of $\ln P_{mb}(E^*/N, V^*/N) = -12$ from the MUBA simulation.

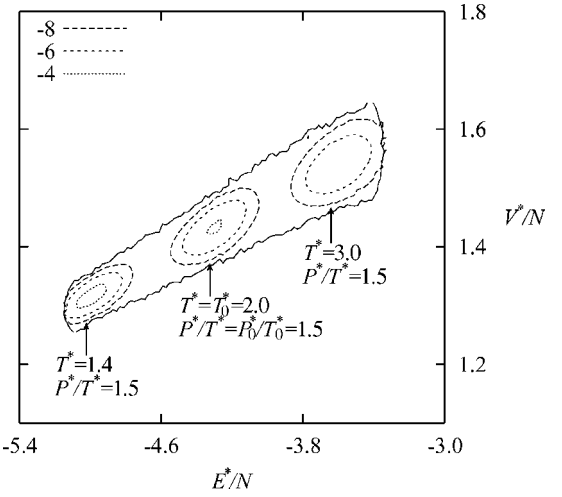

FIG. 6. The contour maps of the probability distributions $P_{NPT}(E^*/N, V^*/N; T^*, P^*)$ in logarithmic scale. They are determined from the MUTH MC simulation by the reweighting techniques at $(T^*, P^*/T^*) = (T_0^*, P_0^*/T_0^*) = (2.0, 1.5)$, $(T^*, P^*/T^*) = (1.4, 1.5)$, and $(T^*, P^*/T^*) = (3.0, 1.5)$. The outer solid curve is the contour map of $\ln P_{mt}(E^*/N, V^*/N) = -12$ from the MUTH simulation.

realize a 1D random walk in the potential-energy space rather than in the volume space. Moreover, the MUBA method is to realize only a 1D random walk in the volume space, whereas the MUBATH algorithm has to perform a 2D random walk. The random walk in the volume space is, therefore, most efficient (most frequent visits to both the lowest and the highest volume values) in the MUBA simulation compared to the MUBATH and the MUTH simulations.

From the broad and wide probability distribution of the long production run from these generalized ISOBATH simulations, various bell-shaped probability distributions $P_{NPT}(E^*/N, V^*/N; T^*, P^*)$ in the ISOBATH ensemble are obtained by the reweighting techniques. They are shown in Figs. 5–7.

From the MUBA simulation, one can obtain ISOBATH distributions at a temperature close to T_0^* and in a wide range of P^*/T^*. Figure 5 shows ISOBATH distributions at $(T^*, P^*/T^*) = (T_0^*, P_0^*/T_0^*) = (2.0, 1.5)$ and at different pressure-temperature ratios $(T_0^*, P^*/T^*) = (2.0, 0.9)$ and $(2.0, 2.4)$. These distributions are inside the broad MUBA distribution $P_{mb}(E^*/N, V^*/N)$ (solid curve in Fig. 5). We can also calculate a distribution at a temperature which is slightly different from T_0^*, although a distribution at a temperature far from T_0^* is out of the MUBA distribution $P_{mb}(E^*/N, V^*/N)$. Note that the histogram reweighting techniques yield accurate results only in the range where we have a sufficient number of entries in the histogram. We, therefore, expect that only the reweighted distributions that lie within the range of the distribution of the MUBA simulation (enclosed in the solid curve in Fig. 5) are reliable. In the present case, the reweighted distributions in the range with $P^*/T^* = 0.9 \sim 2.4$ with $T^* = 2.0$ are expected to be accurate (see the discussions below around Figs. 8–11 for more details).

From the MUTH simulation, one can obtain ISOBATH distributions at T^* and P^* whose ratio P^*/T^* is close to P_0^*/T_0^*. Figure 6 shows ISOBATH distributions at $(T^*, P^*/T^*) = (T_0^*, P_0^*/T_0^*) = (2.0, 1.5)$ and at different temperatures $(T^*, P_0^*/T_0^*) = (1.4, 1.5)$ and $(3.0, 1.5)$. We can also calculate a distribution at a pressure-temperature ratio that is slightly different from P_0^*/T_0^*, although a distribution at P^*/T^* far from P_0^*/T_0^* is out of the MUTH distribution $P_{mt}(E^*/N, V^*/N)$ (solid curve in Fig. 6). In the present case, the reweighted distributions in the range with $T^* = 1.4 \sim 3.0$ with $P^*/T^* = 1.5$ are expected to be accurate.

Figure 7 shows ISOBATH distributions obtained from the MUBATH simulation. These ISOBATH distributions are at

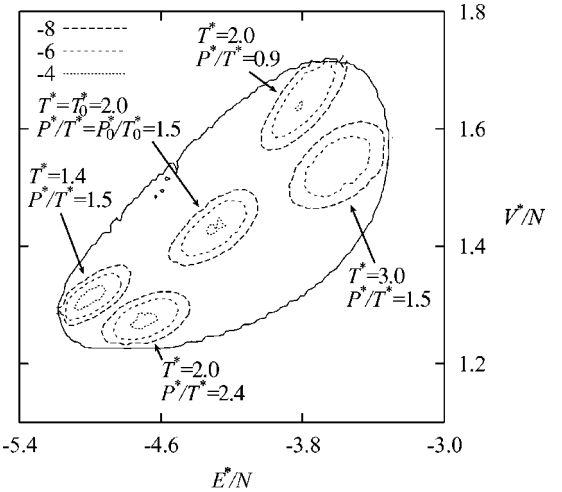

FIG. 7. The contour maps of the probability distributions $P_{NPT}(E^*/N, V^*/N; T^*, P^*)$ in logarithmic scale. They are determined from the MUBATH MC simulation by the reweighting techniques at $(T^*, P^*/T^*) = (T_0^*, P_0^*/T_0^*) = (2.0, 1.5)$, $(T^*, P^*/T^*) = (1.4, 1.5)$, $(T^*, P^*/T^*) = (3.0, 1.5)$, $(T^*, P^*/T^*) = (2.0, 0.9)$, and $(T^*, P^*/T^*) = (2.0, 2.4)$. The outer solid curve is the contour map of $\ln P_{mbt}(E^*/N, V^*/N) = -12$ from the MUBATH simulation.

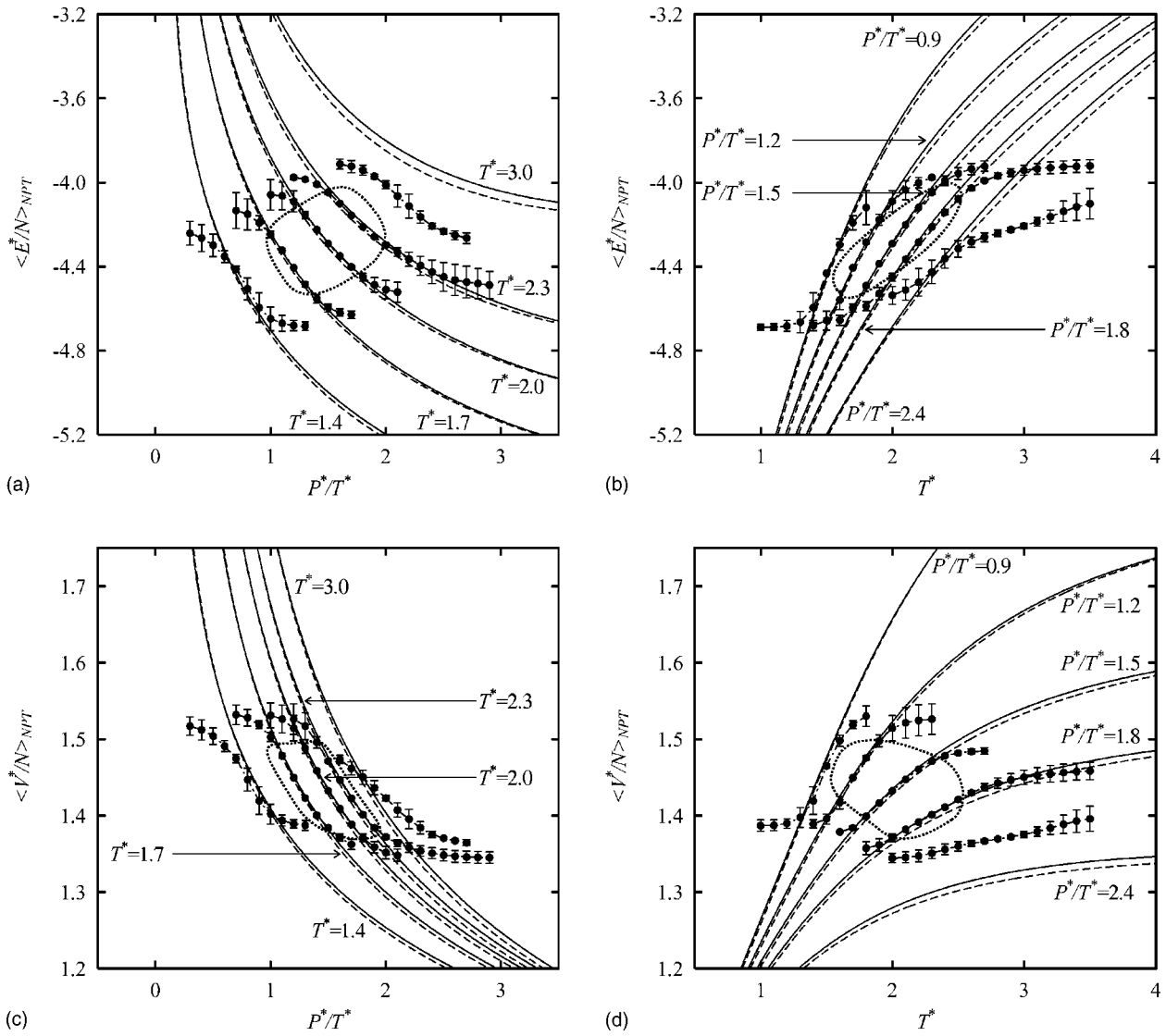

FIG. 8. Average quantity calculation by the ISOBATH MC simulation. Average potential energies per particle $\langle E^*/N\rangle_{NPT}$ (a) as functions of P^*/T^* at several T^* and (b) as functions of T^* at several P^*/T^*. Average volumes per particle $\langle V^*/N\rangle_{NPT}$ (c) as functions of P^*/T^* at several T^* and (d) as functions of T^* at several P^*/T^*. Filled circles: Combination of the ISOBATH MC simulation and the reweighting technique. Solid lines: Equation of states calculated by Johnson, Zollweg, and Gubbins [29]. Broken lines: Equation of states calculated by Sun and Teja [30]. The areas encircled by dotted curves indicate those in which the results by the reweighting techniques agree well with the equations of states.

$(T^*, P^*/T^*) = (T_0^*, P_0^*/T_0^*) = (2.0, 1.5)$, at different pressure-temperature ratios $(T_0^*, P^*/T^*) = (2.0, 0.9)$ and (2.0, 2.4), and at different temperatures $(T^*, P_0^*/T_0^*) = (1.4, 1.5)$ and (3.0, 1.5). This means that the MUBATH simulation enables us to calculate ISOBATH distributions at T^* and P^*/T^* that are significantly different from T_0^* and P_0^*/T_0^*. In the present case, the reweighted distributions in the range with $(T^*, P^*/T^*) = (2.0, 0.9) \sim (2.0, 2.4)$ and $(T^*, P^*/T^*) = (1.4, 1.5) \sim (3.0, 1.5)$ are expected to be accurate.

In order to investigate further the T^* and P^*/T^* ranges in which the ISOBATH and the generalized ISOBATH methods can accurately determine average physical quantities by the reweighting techniques, we show $\langle E^*/N\rangle_{NPT}$ as functions of P^*/T^* in Figs. 8(a), 9(a), 10(a), and 11(a) and as functions of T^* in Figs. 8(b), 9(b), 10(b), and 11(b). We also illustrate $\langle V^*/N^*\rangle_{NPT}$ as functions of P^*/T^* in Figs. 8(c), 9(c), 10(c), and 11(c) and as functions of T^* in Figs. 8(d), 9(d), 10(d), and 11(d). Figure 8 is for the ISOBATH simulation, Fig. 9 is for the MUBA simulation, Fig. 10 is for the MUTH simulation, and Fig. 11 is for the MUBATH simulation. Figures 8–11 also show the curves of two equations of states of the Lennard-Jones 12-6 potential fluid. One was determined by Johnson, Zollweg, and Gubbins [29] and the other by Sun and Teja [30]. In both cases, they calculated the quantities for several pressure- and potential-energy values by the canonical molecular dynamics and MC simulations and fitted the coefficients of the modified Benedict-Webb-Rubin type equation into these simulated data to obtain the equations of states empirically. These curves of equations of states are accurate and can be used as reference in the present work. The areas encircled by dotted curves roughly indicate those

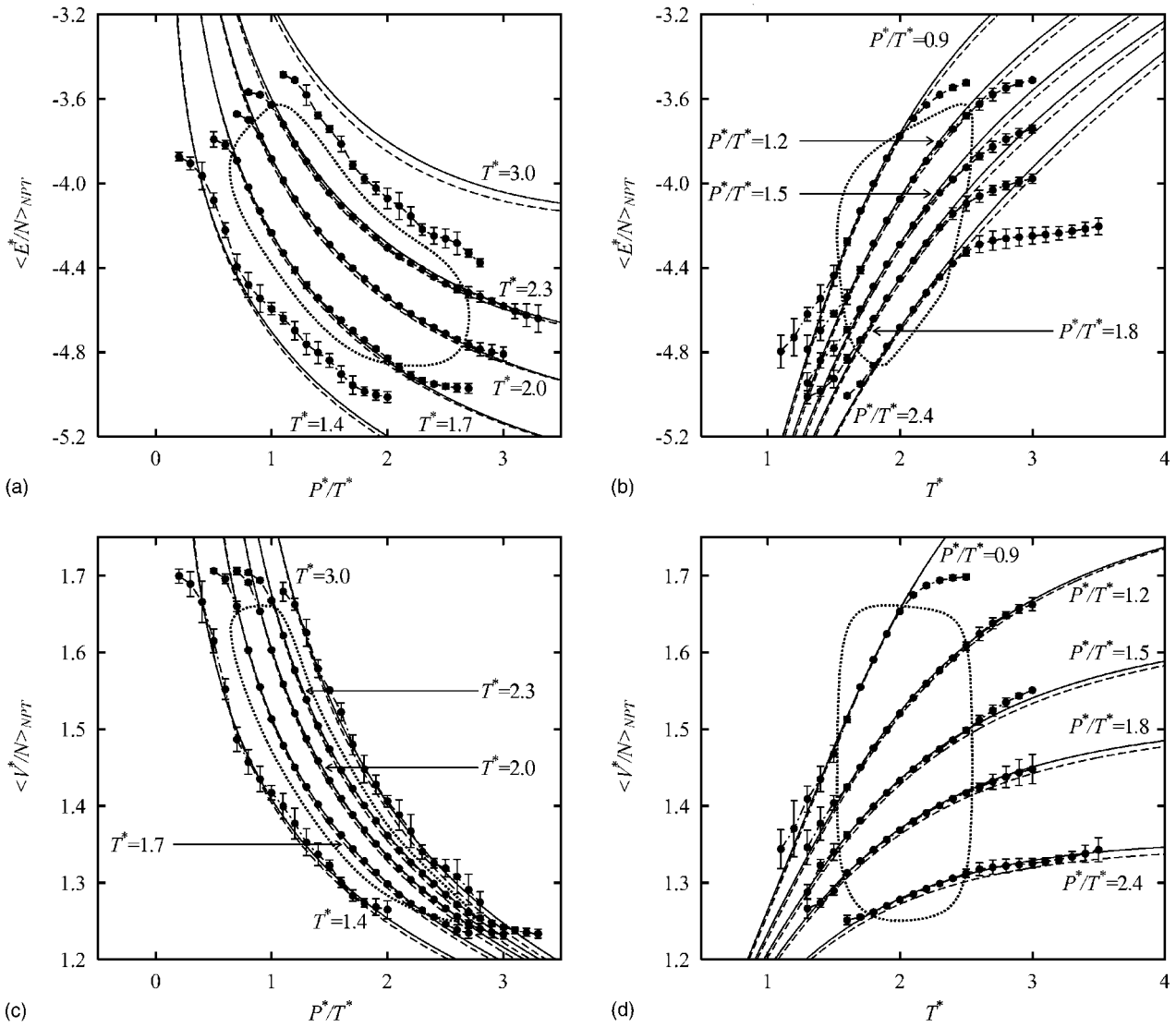

FIG. 9. Average quantity calculation by the MUBA MC simulation. Filled circles: Combination of the MUBA MC simulation and the reweighting techniques. See the caption of Fig. 8 for details.

in which the results by the reweighting techniques agree well with the equations of states.

One cannot calculate physical quantities correctly by combining the ISOBATH algorithm with the reweighting techniques except at T^* and P^*/T^* very close to T_0^* and P_0^*/T_0^*, respectively as shown in Fig. 8. As T^* or P^*/T^* is going far from T_0^* or P_0^*/T_0^*, the error bars of any physical quantities and the deviations from its correct value will get large. The ranges in which $\langle E^*/N\rangle_{NPT}$ and $\langle V^*/N\rangle_{NPT}$ are correct are $1.6 \leqslant T^* \leqslant 2.5$ and $1.0 \leqslant P^*/T^* \leqslant 1.9$. Especially, on the line of $P^*/T^* = P_0^*/T_0^* = 1.5$, $\langle E^*/N\rangle_{NPT}$ and $\langle V^*/N\rangle_{NPT}$ are estimated correctly in the range of $1.8 \leqslant T^* \leqslant 2.3$, and on the line of $T^* = T_0^* = 2.0$, they are correct in the range of $1.3 \leqslant P^*/T^* \leqslant 1.8$. It is necessary to use the generalized ISOBATH methods, such as the MUBATH, MUBA, and MUTH algorithms, to determine physical quantities at T^* and P^*/T^* far from T_0^* and P_0^*/T_0^*. The important point is that one can obtain a desired ISOBATH distribution at numerous temperatures and/or pressures by these generalized ISOBATH algorithms from a single simulation run. This is the outstanding advantage when compared to the conventional ISOBATH MC algorithm, in which simulations have to be carried out separately at each temperature and pressure.

Figure 9 shows $\langle E^*/N\rangle_{NPT}$ and $\langle V^*/N\rangle_{NPT}$ calculated by the MUBA simulation and the reweighting techniques. The areas in which the physical quantities are determined correctly are elongated along T^* = constant lines when compared with the ISOBATH method as shown in Figs. 9(a) and 9(c). Figures 9(b) and 9(d), furthermore, indicate that these areas are elongated vertically at temperatures near T_0^*. These facts imply that the MUBA simulation realizes the volume-space random walk and enables us to calculate physical quantities accurately in the wide range of P^*/T^*. The ranges in which $\langle E^*/N\rangle_{NPT}$ and $\langle V^*/N\rangle_{NPT}$ are correct are $0.7 \leqslant P^*/T^* \leqslant 2.6$. In particular, on the line of $T^* = T_0^* = 2.0$, the reliable area in which physical quantities can be determined accurately by the reweighting techniques is extended to the range of $0.9 \leqslant P^*/T^* \leqslant 2.6$ from the ISOBATH range of $1.3 \leqslant P^*/T^*$

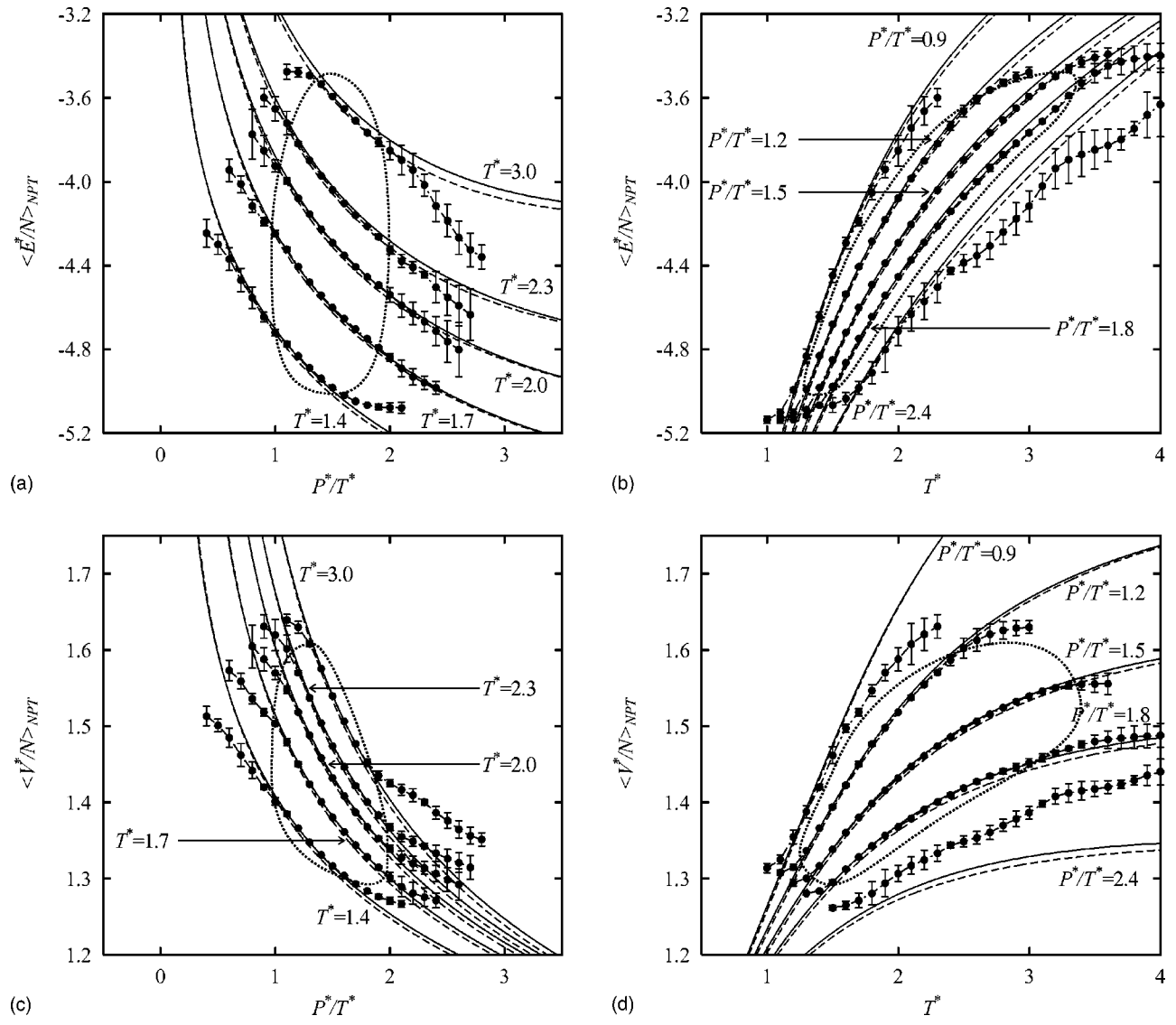

FIG. 10. Average quantity calculation by the MUTH MC simulation. Filled circles: Combination of the MUTH MC simulation and the reweighting techniques. See the caption of Fig. 8 for details.

$\leqslant 1.8$ (see Fig. 8). This P^*/T^* range of the MUBA simulation is more than three times larger than that of the ISOBATH simulation. On the other hand, regarding to T^*, the MUBA simulation has a reliable area for the reweighting techniques that is similar to the ISOBATH simulation. Physical quantities are calculated correctly in the range of $1.6 \leqslant T^* \leqslant 2.5$, essentially the same range as in the ISOBATH simulation.

A similar situation appeared in the MUTH simulation. Figure 10 shows $\langle E^*/N\rangle_{NPT}$ and $\langle V^*/N\rangle_{NPT}$ calculated by the MUTH simulation and the reweighting techniques. The areas in which the physical quantities are determined correctly are elongated along P^*/T^*=constant lines when compared with the ISOBATH method as shown in Figs. 10(b) and 10(d). Figures 10(a) and 10(c), furthermore, indicate that these areas are elongated vertically at pressure-temperature ratios near P_0^*/T_0^*. These facts mean that the MUTH simulation realizes the potential-energy-space random walk and enables us to calculate physical quantities accurately in the wide range of T^*. The ranges in which average quantities are correct are $1.3 \leqslant T^* \leqslant 3.3$. In particular, on the line of $P^*/T^* = P_0^*/T_0^* = 1.5$, the physical quantities are determined correctly in $1.4 \leqslant T^* \leqslant 3.2$. This T^* range is more than three times larger than the ISOBATH simulation range of $1.8 \leqslant T^* \leqslant 2.3$. On the other hand, regarding to P^*/T^*, the MUTH simulation has a similar width to the ISOBATH simulation in which the average values are correct. Physical quantities are calculated correctly in the range of $1.0 \leqslant P^*/T^* \leqslant 1.9$, the same range as in the ISOBATH simulation.

The MUBATH simulation covers the reliable areas for the reweighting techniques applied both to the MUBA simulation and to the MUTH simulation. That is, the MUBATH simulation enables us to calculate physical quantities in wide ranges of both P^*/T^* and T^*. Figure 11 shows that the MUBATH data agree with the equations of states well in $0.1 \leqslant P^*/T^* \leqslant 2.8$ and $1.0 \leqslant T^* \leqslant 3.4$. In particular, they are correct in the range of $1.4 \leqslant T^* \leqslant 3.2$ on the line of $P^*/T^* = P_0^*/T_0^* = 1.5$ and in the range of $0.9 \leqslant P^*/T^* \leqslant 2.6$ on the line

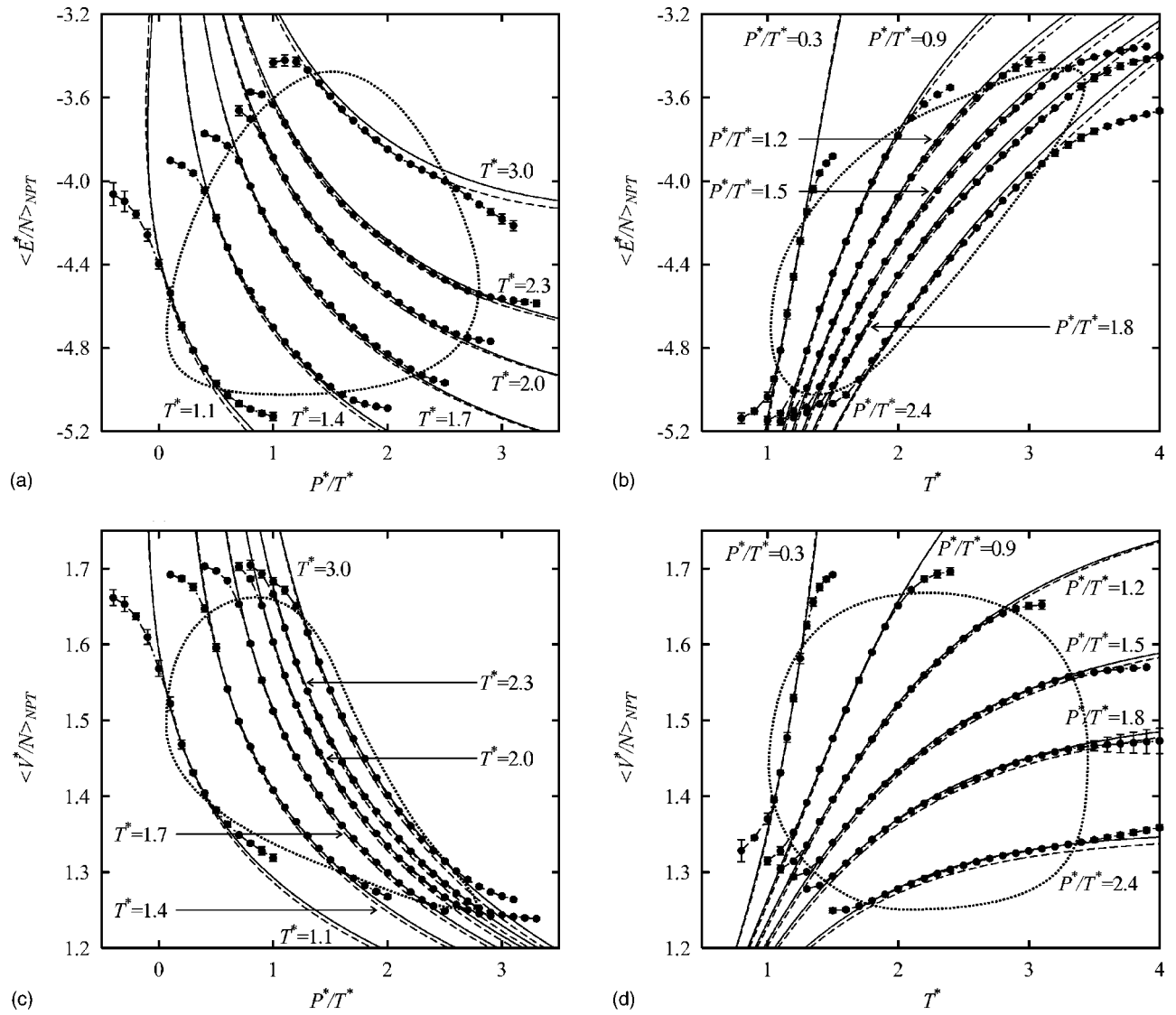

FIG. 11. Average quantity calculation by the MUBATH MC simulation. Filled circles: Combination of the MUBATH MC simulation and the reweighting techniques. See the caption of Fig. 8 for details.

of $T^*=T_0^*=2.0$. These P^*/T^* and T^* ranges are the same as the P^*/T^* range of the MUBA simulation and the T^* range of the MUTH algorithm, respectively. In other words, the MUBATH simulation provides correct average quantities in the ranges of T^* and P^*/T^* more than three times wider than the ISOBATH simulation.

The T^* and P^*/T^* ranges of the encircled areas in Figs. 9–11 agree well with the T^* and P^*/T^* values at which the reweighted ISOBATH distributions are inside the broad distributions of the generalized ISOBATH simulations in Figs. 5–7. For instance, in Fig. 5 the reweighted ISOBATH distributions lie within the original distribution of the MUBA simulation for $P^*/T^*=0.9\sim2.4$ with $T^*=2.0$. This range of P^*/T^* values are consistent with the encircled areas in Fig. 9. In order to estimate T^* and P^*/T^* ranges in which accurate physical quantities are calculated, therefore, one should check that the reweighted ISOBATH distribution is in the original distributions of the generalized ISOBATH simulations. When the reweighted ISOBATH distribution is in the generalized ISOBATH distributions, the physical quantities at these T^* and P^*/T^* values are obtained reliably.

V. CONCLUSIONS

In this paper, we presented three generalized-ensemble MC algorithms, namely the multibaric-multithermal (MUBATH) algorithm, multibaric-isothermal (MUBA) algorithm, and isobaric-multithermal (MUTH) algorithm. We successfully applied these methods to the Lennard-Jones 12-6 potential system. The advantage of our methods is that the simulations sample the configurational space more widely than the conventional ISOBATH MC method. Therefore, one can obtain various ISOBATH ensemble averages from only one simulation run. In principle, the MUBATH simulation can provide various ISOBATH ensemble averages at any T and P/T values. Similarly, the MUBA simulation can provide ISOBATH averages at any P/T and at T near T_0 and the MUTH simulation can provide ISOBATH averages at any T

and at P/T near P_0/T_0. In practice, however, it is impossible to obtain the ideal weight factors with a finite number of iterations for the weight factor determinations. Thus, the reliable ranges of T and P/T in which physical quantities can be determined accurately by the reweighting techniques depend on how much effort one is willing to spend for the weight-factor determinations.

These algorithms will be of use for investigating a large variety of more complex systems, such as proteins, polymers, supercooled liquids, and glasses. It will be also useful to study the problem in which the pressure is important, for example, pressure-induced phase transitions. We will present the results of the applications of the present algorithms to the phase-transition region of the Lennard-Jones potential system in the future communications.

ACKNOWLEDGMENTS

This work was supported, in part, by the Grants-in-Aid for the NAREGI Nanoscience Project and for Scientific Research in Priority Areas, "Water and Biomolecules," from the Ministry of Education, Culture, Sports, Science and Technology, Japan.

[1] N. Metropolis, A. W. Rosenbluth, M. N. Rosenbluth, A. H. Teller, and E. Teller, J. Chem. Phys. **21**, 1087 (1953).
[2] I. R. McDonald, Mol. Phys. **23**, 41 (1972).
[3] M. Creutz, Phys. Rev. Lett. **50**, 1411 (1983).
[4] M. P. Allen and D. J. Tildesley, *Computer Simulation of Liquids* (Clarendon, Oxford, 1987) p. 110.
[5] D. Frenkel and B. Smit, *Understanding Molecular Simulation From Algorithms to Applications* (Academic, San Diego, 2002), p. 111.
[6] U. H. E. Hansmann and Y. Okamoto, in *Ann. Rev. Comput. Phys. VI*, edited by D. Stauffer (World Scientific, Singapore, 1999), p. 129.
[7] A. Mitsutake, Y. Sugita, Y. Okamoto, Biopolymers **60**, 96 (2001).
[8] B. A. Berg, Comput. Phys. Commun. **147**, 52 (2002).
[9] B. A. Berg and T. Neuhaus, Phys. Lett. B **267**, 249 (1991).
[10] B. A. Berg and T. Neuhaus, Phys. Rev. Lett. **68**, 9 (1992).
[11] A. M. Ferrenberg and R. H. Swendsen, Phys. Rev. Lett. **61**, 2635 (1988); **63**, 1658(E) (1989).
[12] H. Okumura and Y. Okamoto, Chem. Phys. Lett. **383**, 391 (2004).
[13] J. Lee, M. A. Novotny, and P. A. Rikvold, Phys. Rev. E **52**, 356 (1995).
[14] S. Kumar, P. Payne, and M. Vásquez, J. Comput. Chem. **17**, 1269 (1996).
[15] C. Bartels and M. Karplus, J. Comput. Chem. **18**, 1450 (1997).
[16] J. Higo, N. Nakajima, H. Shirai, A. Kidera, and H. Nakamura, J. Comput. Chem. **18**, 2086 (1997).
[17] Y. Iba, G. Chikenji, and M. Kikuchi, J. Phys. Soc. Jpn. **67**, 3327 (1998).
[18] Q. Yan, R. Faller, and J. J. de Pablo, J. Chem. Phys. **116**, 8745 (2002).
[19] B. A. Berg, H. Noguchi, and Y. Okamoto, Phys. Rev. E **68**, 036126 (2003).
[20] B. A. Berg and T. Celik, Phys. Rev. Lett. **69**, 2292 (1992).
[21] J. Lee, Phys. Rev. Lett. **71**, 211 (1993); **71**, 2353(E) (1993).
[22] Y. Okamoto and U. H. E. Hansmann, J. Phys. Chem. **99**, 11276 (1995).
[23] H. Okumura and F. Yonezawa, J. Phys. Soc. Jpn. **113**, 9162 (2000).
[24] H. Okumura and F. Yonezawa, J. Phys. Soc. Jpn. **70**, 1006 (2001).
[25] A. Z. Panagiotopoulos, J. Phys.: Condens. Matter **12**, R25 (2000).
[26] J. M. Caillol, J. Chem. Phys. **109**, 4885 (1998).
[27] J. J. Potoff and A. Z. Panagiotopoulos, J. Chem. Phys. **109**, 10914 (1998).
[28] H. Okumura and F. Yonezawa, J. Phys. Soc. Jpn. **70**, 1990 (2001).
[29] J. K. Johnson, J. A. Zollweg, and K. E. Gubbins, Mol. Phys. **78**, 591 (1993).
[30] T. Sun and A. S. Teja, J. Phys. Chem. **100**, 17395 (1996).